

Linear Probing of Molecules at Micrometric Distances from a Surface with Sub-Doppler Frequency Resolution

J. Lukusa Mudiayi,^{1,2} I. Maurin^{1,2}, T. Mashimo,^{1,2} J. C. de Aquino Carvalho^{1,2}, D. Bloch,^{2,1} S. K. Tokunaga,^{1,2} B. Darquié^{2,1} and A. Laliotis^{1,2,*}

¹Laboratoire de Physique des Lasers, Université Sorbonne Paris Nord, F-93430 Villetaneuse, France

²CNRS, UMR 7538, LPL, 99 Avenue J.-B. Clément, F-93430 Villetaneuse, France



(Received 7 February 2021; revised 18 April 2021; accepted 10 June 2021; published 20 July 2021)

We report on precision spectroscopy of subwavelength confined molecular gases. This was obtained by rovibrational selective reflection of NH_3 and SF_6 gases using a quantum cascade laser at $\lambda \approx 10.6 \mu\text{m}$. Our technique probes molecules at micrometric distances ($\approx \lambda/2\pi$) from the window of a macroscopic cell with submegahertz resolution, allowing molecule-surface interaction spectroscopy. We exploit the linearity and high resolution of our technique to gain novel spectroscopic information on the SF_6 greenhouse gas, useful for enriching molecular databases. The natural extension of our work to thin cells will allow compact frequency references and improved measurements of the Casimir-Polder interaction with molecules.

DOI: [10.1103/PhysRevLett.127.043201](https://doi.org/10.1103/PhysRevLett.127.043201)

High-resolution molecular spectroscopy in gas cells has far-reaching applications ranging from Earth and atmospheric sciences [1,2] to astrophysics [3], metrology and frequency referencing [4–7], gas sensing, and trace detection [8], as well as fundamental physics measurements [9–13]. The growing demand for miniaturization has led to the fabrication of compact platforms that interface molecular gases with solid-state devices, such as on-chip waveguides [6], hollow core fibers [5], porous media [14], and thin cells [15]. However, the above experiments typically operate at high gas pressures due to low transition probabilities of molecular lines, and the resolution is limited by either pressure or Doppler broadening. Therefore, achieving precision spectroscopy of a confined molecular gas is challenging.

Confined gases have been studied primarily with atomic alkali vapors with implications ranging from fundamental physics to quantum technologies. Thin cells have been used to study the Dicke narrowing effect [16], allowing high-resolution sub-Doppler linear spectroscopy [17] and, more recently, investigations of dipole-dipole interactions with high-density atomic vapors [18]. Probing Rydberg atoms in thin cells is also a promising approach for quantum information processing [19]. Three-dimensional atomic confinement has also been explored with photonic crystals [20] or random media [21]. Finally, the fundamental Casimir-Polder interaction has been studied with confined atomic vapors, either in nanometric thin cells [22] or by selective reflection spectroscopy [23].

High-resolution spectroscopy of confined molecules offers attractive prospects for fabricating compact frequency references. Additionally, it paves the way for spectroscopic probing of the Casimir-Polder molecule-

surface interaction, a topic of interest for physical-chemistry or atmospheric sciences [24,25], as well as for fundamental physics due to the rich geometry of polyatomic molecules. The dependence of the Casimir-Polder interaction on molecular orientation (anisotropy) [25–27] or on molecular chirality [28] (when the surface is also chiral) are, for instance, open theoretical questions. Although molecule-surface interactions are of fundamental interest, so far experimental tests are few, and comparison with theoretical predictions has been challenging [29–33].

One possible way for probing molecular gases close to a dielectric surface, in an effectively confined environment, is via selective reflection in a molecular gas cell [34,35]. Frequency-modulated selective reflection spectroscopy (FMSR), under normal incidence, is sensitive to particles (molecules or atoms) that move parallel to the dielectric window of the gas cell at distances comparable to the reduced wavelength of excitation ($\tilde{\lambda} = \lambda/2\pi$). This feature has made FMSR an important spectroscopic technique for measuring Casimir-Polder interactions with excited state atoms [36,37]. Additionally, FMSR is a linear spectroscopy without crossover resonances that often muddle saturated absorption spectra. This allows easy interpretation of observed line shapes and the study of gas properties, such as collisional shifts and broadenings [37–40], even at high densities where volume absorption spectroscopy is unfeasible. The above advantages of FMSR can have an important impact for molecular spectroscopy [1–3,8,41–43], allowing simultaneous measurements of transition frequencies, intensities, and collisional broadenings. Although attempts have been made to probe alkali dimers [44] at high temperatures, high-resolution FMSR has so far been exclusively performed on atomic vapors.

Here, we perform high-resolution rovibrational FMSR of NH_3 and SF_6 gases at $\lambda \approx 10.6 \mu\text{m}$. Our experiment probes molecules at a depth of about $\lambda \approx 1.7 \mu\text{m}$ with a sub-megahertz resolution, limited by the linewidth of our quantum cascade laser (QCL) source. The exceptional combination of linearity and high resolution offered by selective reflection is used to resolve the hyperfine structure of NH_3 and gain novel spectroscopic information on the SF_6 molecule, of importance to atmospheric physics and corresponding molecular databases. Finally, we use FMSR to perform molecule-surface interaction spectroscopy with a sensitivity in Casimir-Polder shifts of about 10 kHz at $1 \mu\text{m}$ from the surface.

Selective reflection is performed on a gas cell at room temperature constructed out of metallic vacuum tubes with ZnSe windows. We use a commercial QCL, of output power $\approx 5 \text{ mW}$, whose frequency is scanned by changing the laser current. A frequency modulation (FM) is applied at $f_{\text{FM}} \approx 8 \text{ kHz}$ with a peak-to-peak amplitude $M \approx 0.5 \text{ MHz}$. The reflection from the gas-window interface (Fig. 1) is demodulated at frequency f_{FM} with a lock-in amplifier. In the limit $M \ll \Gamma$, where Γ is the homogeneous linewidth, this provides the derivative of the direct signal and increases the contrast of the sub-Doppler contribution originating from molecules that are slow in the direction of the beam [36]. To avoid any residual Doppler broadening, selective reflection is performed at normal incidence. When $\Gamma \ll \Delta_D$, where Δ_D is the Doppler full width at half maximum (FWHM), the selective reflection signal demodulated at the FM frequency (S_{FMSR}) becomes a dispersive Lorentzian curve of width equal to Γ [38]:

$$S_{\text{FMSR}} \propto -\mu^2 M \frac{N \lambda}{\Gamma u_p} \frac{2\delta/\Gamma}{1 + (2\delta/\Gamma)^2}. \quad (1)$$

Here, μ is the dipole moment matrix element of the probed transition, N is the population of the lower state, u_p is the most probable molecular velocity in the direction of the beam, and δ is the laser detuning.

We focus on NH_3 and SF_6 molecules with strong rovibrational transitions in the midinfrared ($\approx 10.6 \mu\text{m}$) window. Ammonia (NH_3) is of tetrahedral geometry with

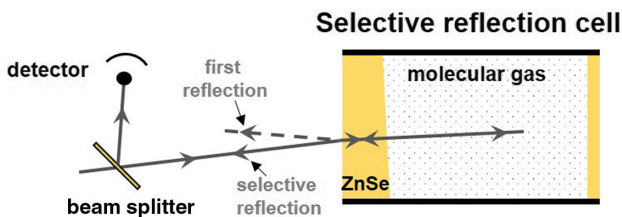


FIG. 1. Schematic of the selective reflection measurement. The wedged window allows separation of the selective reflection beam (solid line at normal incidence) from the first reflection (dashed line).

widely spaced rotational levels. The only major line of the most abundant ammonia isotope within the 150 GHz spectral window of our laser is the saP(1,0) rovibrational transition at 28,427,281.4 MHz [45], from the ground state to the first ν_2 vibration. The spread of the observed hyperfine structure, resulting from electric quadrupole interactions in the lower level, is a few megahertz [46] (Fig. 2) and is unresolved with Doppler-limited resolution ($\Delta_D = 85 \text{ MHz}$ at room temperature). Sulfur hexafluoride (SF_6) is of spherical geometry, presenting a multitude of transitions of the ν_3 vibrational mode in the frequency range of our laser with a superfine structure occasionally resolved even with Doppler-limited resolution ($\Delta_D = 29 \text{ MHz}$ at room temperature) [47,48].

A saturated absorption setup provides a molecular frequency reference in the volume at low gas pressure, allowing a frequency calibration of our scans. Saturated absorption (S_{SA}) is recorded simultaneously with selective reflection and is demodulated with a lock-in amplifier at f_{FM} or $2f_{\text{FM}}$. $2f_{\text{FM}}$ demodulation provides a better contrast of the narrow peaks at the expense of signal amplitude [49]. The frequency drift of the free-running QCL is incompatible with high-resolution spectroscopy. We thus use an auxiliary setup to lock the laser frequency either on the side of a direct absorption profile or at the slope of the first derivative of the linear absorption of the ammonia saP(1,0) transition. The laser frequency is then scanned by adding an offset to the error signal. The laser stabilization circuit corrects only the slow laser frequency drift (timescale $> 1 \text{ ms}$) and not the laser linewidth.

Figure 2 shows selective reflection spectra of ammonia demodulated at f_{FM} (S_{FMSR}) and normalized to the off-resonant reflection of the gas-window interface (S_R^0) at pressures from $P = 25 \text{ mTorr}$ to $P = 200 \text{ mTorr}$. The saturated absorption frequency reference (S_{SA}) is shown in Fig. 2(a). The hyperfine structure of the lower rovibrational level and crossover resonances are visible on the saturated absorption spectrum, typically recorded at $P = 15 \text{ mTorr}$. The hyperfine structure of ammonia is also resolved by FMSR for pressures lower than $\approx 50 \text{ mTorr}$ [Figs. 2(c) and 2(d)]. However, unlike for saturated absorption spectroscopy, there are no crossover resonances and the ratio between the amplitudes of each $F \rightarrow F'$ hyperfine transition is defined by its theoretical estimated strength (1:5:3 for $0 \rightarrow 1$, $2 \rightarrow 1$, $1 \rightarrow 1$, respectively [46]). The FMSR signals in Fig. 2 are the result of averaging 40 individual ≈ 2 -min-long scans.

The frequency resolution of both saturated absorption and FMSR is determined by the laser linewidth, pressure broadening, and FM excursion, whereas power and transit-time broadening have a minor effect in these conditions. The laser linewidth is $\approx 0.6 \text{ MHz}$ FWHM, experimentally measured by examining the saturated absorption linewidth while reducing FM distortions and pressure broadening [56]. At low molecular pressures, laser linewidth is the

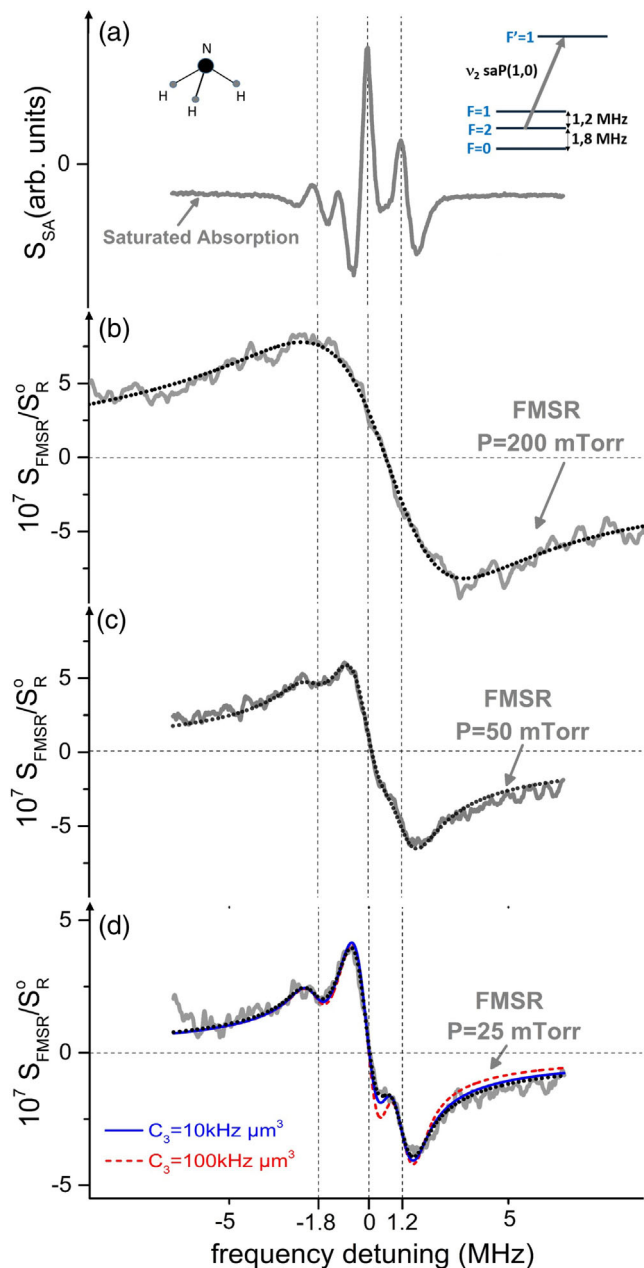


FIG. 2. NH₃ spectroscopy. (a) Saturated absorption frequency reference (S_{SA}) at $P = 15$ mTorr (demodulated at $2f_{FM}$). (b)–(d) FMSR signal, normalized to off-resonant reflection (S_{FMSR}/S_R^0) at $P = 200$ mTorr, $P = 50$ mTorr, and $P = 25$ mTorr, respectively. The FM amplitude is $M \approx 0.5$ MHz. Black dotted lines are fits of a theoretical model including the effects of frequency modulation and laser linewidth. In (d), we also show fits including molecule-surface interactions with $C_3 = 10 \text{ kHz } \mu\text{m}^3$ (solid blue line) and $C_3 = 100 \text{ kHz } \mu\text{m}^3$ (dashed red line). Top right: level structure of the ν_2 saP(1,0) rovibration. The frequency of hyperfine transitions is indicated as dashed vertical lines.

frequency resolution limit for both techniques in the current setup.

At sufficiently high pressures, the FMSR signal linewidth is dominated by collisional broadening which is

proportional to gas pressure. In this case, the FMSR amplitude ($\approx 10^{-6}$) remains constant with pressure, because the reduction of lower state population is compensated by the decrease of transition linewidth [the ratio N/Γ in Eq. (1) stays constant]. This is seen in Figs. 2(b) and 2(c) and was also verified for ammonia pressures as high as a few Torr [56]. The loss of FMSR signal amplitude at lower pressures is a consequence of the laser linewidth-limited frequency resolution [Fig. 2(d)]. In the experimental conditions in Fig. 2, the saturated absorption amplitude is more than 1 order of magnitude larger than FMSR; however, the pressure range of saturated absorption is limited, mainly because the saturation intensity increases with transition linewidth.

The black dotted curves in Fig. 2 show the predicted FMSR line shapes, including the exact FM line shape distortion [36] [beyond the assumptions of Eq. (1)] and the effects of laser linewidth, considered to be a Gaussian function of ≈ 0.6 MHz FWHM. The curves are adjusted for an overall amplitude (the ratio of the hyperfine components is fixed to its theoretical value), a collisional linewidth and shift (compared to the saturated absorption reference), and an offset. The deduced pressure broadening is about 27 MHz/Torr (FWHM) consistent with other values reported in the literature [57], while the shift between FMSR and saturated absorption remains negligible.

We also use FMSR in order to measure molecule-surface, Casimir-Polder interactions. In Fig. 2(d), we show the theoretical spectra including molecule-surface interaction effects [36], adjusted for an overall amplitude and offset (blue and dashed red curves, respectively). We assume a $-C_3/z^3$ potential, where z is the molecule-surface distance and C_3 is the spectroscopic van der Waals coefficient (the difference between C_3 coefficients of the probed states). Our FMSR spectroscopic Casimir-Polder measurement gives an upper bound of $\approx 10 \text{ kHz } \mu\text{m}^3$ to the C_3 coefficient. Systematic errors are reduced by the elimination of a parasitic background and laser frequency drift. There are no theoretical calculations for the spectroscopic C_3 of ammonia that depend on the allowed electronic and vibrational contributions [32,58] and on the anisotropy due to the molecular rotation [27]. Nevertheless, based on previous calculations for other molecules [27,32,58], we estimate that C_3 should be less than $1 \text{ kHz } \mu\text{m}^3$. We note that Casimir-Polder retardation can also play a role in such experiments [58]. The sensitivity of dedicated molecule-surface FMSR spectroscopy can be improved by reducing the QCL linewidth [59–61] or by probing smaller wavelength transitions. For more details, see Supplemental Material [49].

We subsequently expanded our studies to SF₆ for which molecular databases are incomplete [41], because its dense rovibrational spectrum is difficult to resolve with traditional Fourier transform spectroscopy. High-resolution saturated absorption measurements of SF₆ have also been performed

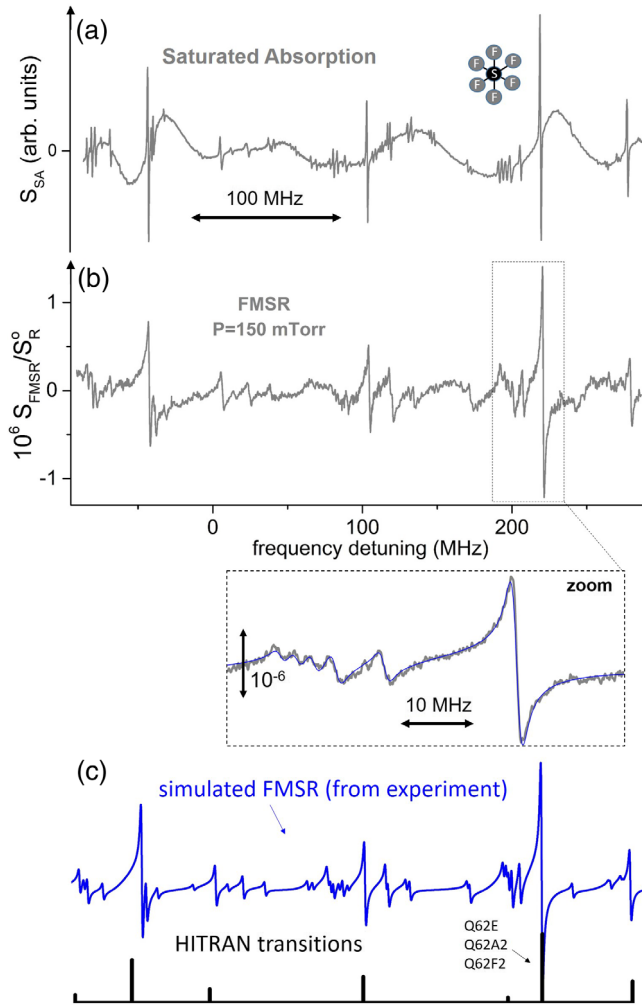


FIG. 3. SF_6 spectroscopy. (a) Saturated absorption frequency reference (S_{SA}) at $P = 15$ mTorr (demodulated at f_{FM}). (b) FMSR signal, normalized to off-resonant reflection (S_{FMSR}/S_R^0) at $P = 150$ mTorr with FM amplitude $M = 0.5$ MHz. The frequency scale is centered on the saP(0,1) transition of ammonia. The spectrum is a patch of curves from eight different regions each covering about 30–40 MHz. The curve of each region results from averaging 40 individual ≈ 2 min scans. An enlargement of the FMSR scan is also shown around the Q62E, Q62A2, and Q62F2 SF_6 transitions of the ν_3 vibrational mode, predicted to be degenerate at 28427502.6 MHz, in the HITRAN database [45]. A fit of the enlarged selective reflection spectra is shown as a blue solid line. (c) Predicted selective reflection spectrum using the SF_6 transition positions and amplitudes extracted from the FMSR experiment (solid blue line). The positions and amplitudes of the HITRAN listed rovibrations [45] are also shown as vertical black lines.

with CO_2 lasers. However, these measurements were strongly limited to the parts of the $10.6 \mu m$ spectrum [47,48] that are accessible with CO_2 sources. Here, we perform selective reflection spectroscopy on SF_6 rovibrations in the previously unexplored frequency range centered around the saP(0,1) transition of ammonia.

Figure 3 shows normalized FMSR spectra of SF_6 at 150 mTorr, along with a saturated absorption reference at 15 mTorr. The HITRAN database is incomplete for SF_6 transitions [45]. We therefore used a Bristol Instruments wavelength meter with a relative frequency uncertainty of ≈ 5 MHz to pinpoint the frequency positions of the SF_6 rovibrations. Long frequency scans, such as the ≈ 300 MHz scan in Fig. 3, can suffer from an oscillating background due to interference of the selective reflection signal with other parasitic reflections originating from various parts of the setup. In order to reduce this background, we have used a system of electronic valves allowing us to empty and refill the chamber with molecules within tens of seconds and detect the difference between the two signals. Using this technique, the interferometric background is reduced to values below 2×10^{-7} [49].

The saturated absorption spectrum provides a higher signal to noise ratio; however, the transition amplitudes cannot be easily extracted due to nonlinearity, differential saturation between lines, and the possible existence of crossover resonances. Conversely, the amplitudes of the resolved molecular transitions can be extracted using linear selective reflection (FMSR). For this purpose, we perform many local fits [see enlargement in Fig. 3(b)], delimiting a small part of the selective reflection spectrum, to minimize the effects of the interferometric background. The fits provide the relative amplitude, frequency position, and pressure broadened linewidth of the transitions. Here, the effects of molecule-surface interactions are ignored. The uncertainty on the relative transition amplitudes depends on the short-term noise of our experiment, which is smaller than 10^{-7} [Fig. 3(b)]. This translates to $\approx 10\%$ uncertainty for the strongest transitions [49]. Further improvements can be made by increasing the scan integration time. Within the resolution of our experiment (limited by laser linewidth), no collisional frequency shift is measurable between the positions obtained by FMSR and saturated absorption. The final simulated spectrum is shown in Fig. 3(c) (solid blue curve). For comparison, we also show the positions and amplitudes of SF_6 transitions listed in the HITRAN database [45] (black bars). The HITRAN data are insufficient to interpret our experimental curves. Further information can be gained by extending our measurements in the entire spectrum of the ν_3 rovibration of SF_6 .

Accurate determination of transition amplitudes and positions in laboratory experiments is crucial in atmospheric physics applications, in particular, for monitoring gas concentrations by remote sensing experiments [1,2]. Measuring the atmospheric abundance of SF_6 , an important greenhouse gas, is essential for monitoring global warming [41,42]. However, SF_6 and other heavy atmospheric species ($ClONO_2$, CF_4 , ...) with low-lying vibrational modes exhibit both a dense rotational structure and many hot bands, and traditional Fourier transform infrared spectra do not show isolated lines but rather unresolved clusters of

many transitions. For such species, molecular databases neglect many significant hot bands, feature inaccurate intensities, and cannot be exploited for atmospheric quantification [41,43]. In this respect, selective reflection spectroscopy which combines linearity and crossover-transition-free sub-Doppler resolution could be useful, offering complementary information on transition amplitudes and positions for heavy atmospheric molecules.

In conclusion, we have performed high-resolution, linear spectroscopy of gas phase molecules at micrometric distances away from a surface. The achieved resolution is ≈ 0.6 MHz limited by the laser linewidth but can be further improved by locking the QCL to a more stable frequency source [59–61]. We demonstrate the advantages of this technique for enriching molecular databases and for molecule-surface interaction spectroscopy.

This work, and its natural extension to molecular thin cells of subwavelength thickness, paves the way toward the following. (i) The fabrication of simple and compact molecular frequency references throughout the spectrum without resorting to saturated absorption schemes, required in fiber platforms [62–64]. Multiple cells [65] or multipass techniques can increase the signal of such devices without compromising their compactness. (ii) The measurement of the molecule-surface interaction in nanometric thin cells that allow us to control molecular confinement by changing cell thickness [22]. Probing molecule-surface interactions using rovibrational spectroscopy can be promising for measurement of the Casimir-Polder anisotropy [26]. This is because light-induced transitions tend to orient the molecule along the electric field of the probing beam [27], while the electronic cloud remains in its ground state. Additionally, the interaction of molecules with near-field thermal emission [66–68] can be a point of interest, as molecular rovibrational energy can be comparable to the thermal energy even at room temperatures. Finally, molecular electronic transitions can be used for exploring chirality effects [28]. (iii) Exploring the fundamental physics of subwavelength confinement with molecules. This includes studies of the Maxwell-Boltzmann distribution close to surfaces with narrow velocity selection [69,70], studies of superradiance with molecules [71], or studies of local field corrections [18,39,72] with high-density molecular gases. In this respect, the flexibility of molecular cells that operate at room temperature with independent control of gas pressure can be an additional advantage compared to atomic vapors.

We thank J. R. Rios Leite and M. Ducloy for discussions and A. Shelkovich and J. Grucker for participating in preliminary measurements. We acknowledge financial support from the ANR project SQUAT (Grant No. ANR-20-CE92-0006-01), PVCM (Grant No. ANR-15-CE30-0005-01), Ile-de-France region (DIM-NanoK), and the LABEX Cluster of Excellence FIRST-TF

(ANR-10-LABX-48-01). T. M. was funded by Chuo University of Tokyo.

*laliotis@univ-paris13.fr

- [1] O. L. Polyansky, K. Bielska, M. Ghysels, L. Lodi, N. F. Zobov, J. T. Hodges, and J. Tennyson, *Phys. Rev. Lett.* **114**, 243001 (2015).
- [2] A. Vaskuri, P. Kärhä, L. Egli, J. Gröbner, and E. Ikonen, *Atmos. Meas. Tech.* **11**, 3595 (2018).
- [3] E. Roueff, S. Sahal-Bréchet, M. S. Dimitrijevi, N. Moreau, and H. Abgrall, *Atoms* **8**, 36 (2020).
- [4] S. L. Gilbert, W. C. Swann, and T. Dennis, in *Laser Frequency Stabilization, Standards, Measurement, and Applications* edited by J. L. Hall and J. Ye, International Society for Optics and Photonics (SPIE, Bellingham, WA, 2001), Vol. 4269, pp. 184–191, <https://doi.org/10.1117/12.424468>.
- [5] F. Benabid, F. Couny, J. C. Knight, T. A. Birks, and P. S. J. Russell, *Nature (London)* **434**, 488 (2005).
- [6] R. Zektzer, M. T. Hummon, L. Stern, Y. Sebbag, Y. Barash, N. Mazurski, J. Kitching, and U. Levy, *Laser Photonics Rev.* **14**, 1900414 (2020).
- [7] R. Santagata, D. B. A. Tran, B. Argence, O. Lopez, S. K. Tokunaga, F. Wiotte, H. Mouhamad, A. Goncharov, M. Abgrall, Y. Le Coq, H. Alvarez-Martinez, R. Le Targat, W. K. Lee, D. Xu, P.-E. Pottie, B. Darquié, and A. Amy-Klein, *Optica* **6**, 411 (2019).
- [8] I. Galli, S. Bartalini, R. Ballerini, M. Barucci, P. Cancio, M. D. Pas, G. Giusfredi, D. Mazzotti, N. Akikusa, and P. D. Natale, *Optica* **3**, 385 (2016).
- [9] C. Daussy, M. Guinet, A. Amy-Klein, K. Djerroud, Y. Hermier, S. Briaudeau, C. J. Bordé, and C. Chardonnet, *Phys. Rev. Lett.* **98**, 250801 (2007).
- [10] L. Moretti, A. Castrillo, E. Fasci, M. D. De Vizia, G. Casa, G. Galzerano, A. Merlone, P. Laporta, and L. Gianfrani, *Phys. Rev. Lett.* **111**, 060803 (2013).
- [11] C. Daussy, T. Marrel, A. Amy-Klein, C. T. Nguyen, C. J. Bordé, and C. Chardonnet, *Phys. Rev. Lett.* **83**, 1554 (1999).
- [12] M. L. Diouf, F. M. J. Cozijn, K.-F. Lai, E. J. Salumbides, and W. Ubachs, *Phys. Rev. Research* **2**, 023209 (2020).
- [13] A. Cournol *et al.*, *Quantum Electron.* **49**, 288 (2019).
- [14] T. Svensson, E. Adolffson, M. Lewander, C. T. Xu, and S. Svanberg, *Phys. Rev. Lett.* **107**, 143901 (2011).
- [15] J.-M. Hartmann, X. Landsheere, C. Boulet, D. Sarkisyan, A. S. Sarkisyan, C. Leroy, and E. Panguì, *Phys. Rev. A* **93**, 012516 (2016).
- [16] R. H. Romer and R. H. Dicke, *Phys. Rev.* **99**, 532 (1955).
- [17] G. Dutier, A. Yarovitski, S. Saltiel, A. Papoyan, D. Sarkisyan, D. Bloch, and M. Ducloy, *Europhys. Lett.* **63**, 35 (2003).
- [18] T. Peyrot, Y. R. P. Sortais, A. Browaeys, A. Sargsyan, D. Sarkisyan, J. Keaveney, I. G. Hughes, and C. S. Adams, *Phys. Rev. Lett.* **120**, 243401 (2018).
- [19] F. Ripka, H. Kübler, R. Löw, and T. Pfau, *Science* **362**, 446 (2018).
- [20] P. Ballin, E. Moufarej, I. Maurin, A. Laliotis, and D. Bloch, *Appl. Phys. Lett.* **102**, 231115 (2013).

- [21] S. Villalba, H. Failache, A. Laliotis, L. Lenci, S. Barreiro, and A. Lezama, *Opt. Lett.* **38**, 193 (2013).
- [22] M. Fichet, G. Dutier, A. Yarovitsky, P. Todorov, I. Hamdi, I. Maurin, S. Saltiel, D. Sarkisyan, M.-P. Gorza, D. Bloch, and M. Ducloy, *Europhys. Lett.* **77**, 54001 (2007).
- [23] D. Bloch and M. Ducloy, in *Advances In Atomic, Molecular, and Optical Physics* edited by B. Bederson and H. Walther (Academic Press, New York, 2005), Vol. 50, Chap. Atom-wall interaction, pp. 91–154, [https://doi.org/10.1016/S1049-250X\(05\)80008-4](https://doi.org/10.1016/S1049-250X(05)80008-4).
- [24] J. Fiedler, D. F. Parsons, F. A. Burger, P. Thiyam, M. Walter, I. Brevik, C. Persson, S. Y. Buhmann, and M. Boström, *Phys. Chem. Chem. Phys.* **21**, 21296 (2019).
- [25] M. Antezza, I. Fialkovsky, and N. Khusnutdinov, *Phys. Rev. B* **102**, 195422 (2020).
- [26] P. Thiyam, P. Parashar, K. V. Shajesh, C. Persson, M. Schaden, I. Brevik, D. F. Parsons, K. A. Milton, O. I. Malyi, and M. Boström, *Phys. Rev. A* **92**, 052704 (2015).
- [27] G. Bimonte, T. Emig, R. L. Jaffe, and M. Kardar, *Phys. Rev. A* **94**, 022509 (2016).
- [28] D. T. Butcher, S. Y. Buhmann, and S. Scheel, *New J. Phys.* **14**, 113013 (2012).
- [29] A. Shih, D. Raskin, and P. Kusch, *Phys. Rev. A* **9**, 652 (1974).
- [30] D. Raskin and P. Kusch, *Phys. Rev.* **179**, 712 (1969).
- [31] M. Boustimi, J. Baudon, F. Pirani, M. Ducloy, J. Reinhardt, F. Perales, C. Mainos, V. Bocvarski, and J. Robert, *Europhys. Lett.* **56**, 644 (2001).
- [32] C. Brand, J. Fiedler, T. Juffmann, M. Sclafani, C. Knobloch, S. Scheel, Y. Lilach, O. Cheshnovsky, and M. Arndt, *Ann. Phys. (Berlin)* **527**, 580 (2015).
- [33] C. Wagner, N. Fournier, V. G. Ruiz, C. Li, K. Müllen, M. Rohlfing, A. Tkatchenko, R. Temirov, and F. S. Tautz, *Nat. Commun.* **5**, 5568 (2014).
- [34] J. Woerdman and M. Schuurmans, *Opt. Commun.* **14**, 248 (1975).
- [35] M. F. H. Schuurmans, *J. Phys. France* **37**, 469 (1976).
- [36] M. Ducloy and M. Fichet, *J. Phys. II* **1**, 1429 (1991).
- [37] M. Chevrollier, M. Fichet, M. Oria, G. Rahmat, D. Bloch, and M. Ducloy, *J. Phys. II France* **2**, 631 (1992).
- [38] A. M. Akul'shin, V. L. Velichanskii, A. S. Zibrov, V. V. Nikitin, V. V. Sautenkov, E. K. Yurkin, and N. V. Senkov, *JETP Lett.* **36**, 303 (1982).
- [39] V. Vuletic, V. Sautenkov, C. Zimmermann, and T. Hänsch, *Opt. Commun.* **99**, 185 (1993).
- [40] A. Laliotis, I. Maurin, M. Fichet, D. Bloch, M. Ducloy, N. Balasanyan, A. Sarkisyan, and D. Sarkisyan, *Appl. Phys. B* **90**, 415 (2008).
- [41] M. Faye, L. Manceron, P. Roy, V. Boudon, and M. Loëte, *J. Mol. Spectrosc.* **348**, 37 (2018).
- [42] M. A. K. Khalil, *Annu. Rev. Energy Environ.* **24**, 645 (1999).
- [43] J. Krieg, J. Nothholt, E. Mahieu, C. Rinsland, and R. Zander, *J. Quant. Spectrosc. Radiat. Transfer* **92**, 383 (2005).
- [44] S. Shmavonyan, A. Khanbekyan, A. Gogyan, M. Movsisyan, and A. Papoyan, *J. Mol. Spectrosc.* **313**, 14 (2015).
- [45] I. Gordon *et al.*, *J. Quant. Spectrosc. Radiat. Transfer* **203**, 3 (2017).
- [46] S. Urban, F. Herlemont, M. Khelkhal, H. Fichoux, and J. Legrand, *J. Mol. Spectrosc.* **200**, 280 (2000).
- [47] B. Bobin, C. J. Bordé, J. Bordé, and C. Bréant, *J. Mol. Spectrosc.* **121**, 91 (1987).
- [48] O. Acef, C. J. Bordé, A. Clairon, G. Pierre, and B. Sartakov, *J. Mol. Spectrosc.* **199**, 188 (2000).
- [49] See Supplemental Material at <http://link.aps.org/supplemental/10.1103/PhysRevLett.127.043201> for details on experimental techniques, sulfur hexafluoride spectroscopy, molecule-surface interaction measurements, and calculations of selective reflection signal, which includes Refs. [50–55].
- [50] C. Lemarchand, M. Triki, B. Darquié, C. J. Bordé, C. Chardonnet, and C. Daussy, *New J. Phys.* **13**, 073028 (2011).
- [51] Y. Kosichkin, A. Nadezhdinskii, and E. Stepanov, *J. Quant. Spectrosc. Radiat. Transfer* **43**, 499 (1990).
- [52] O. D. Lorenzo-Filho, P. C. de Oliveira, and J. R. R. Leite, *Opt. Lett.* **16**, 1768 (1991).
- [53] P. Pracna, V. Spirko, and W. Kraemer, *J. Mol. Spectrosc.* **136**, 317 (1989).
- [54] K. Kim, R. S. McDowell, and W. T. King, *J. Chem. Phys.* **73**, 36 (1980).
- [55] N. Papageorgiou, M. Fichet, V. Sautenkov, D. Bloch, and M. Ducloy, *Laser Phys.* **4**, 392 (1994).
- [56] J. Lukusa Mudiayi, Spectroscopie de réflexion sélective sur des raies rovibrationnelles moléculaires, Ph.D. thesis, Université de Paris 13, 2019, <https://hal.archives-ouvertes.fr/tel-03250753v1>.
- [57] S. Mejri, P. L. T. Sow, O. Kozlova, C. Ayari, S. K. Tokunaga, C. Chardonnet, S. Briaudeau, B. Darquié, F. Rohart, and C. Daussy, *Metrologia* **52**, S314 (2015).
- [58] S. Y. Buhmann, S. Scheel, S. A. Ellingsen, K. Hornberger, and A. Jacob, *Phys. Rev. A* **85**, 042513 (2012).
- [59] F. Cappelli, I. Galli, S. Borri, G. Giusfredi, P. Cancio, D. Mazzotti, A. Montori, N. Akikusa, M. Yamanishi, S. Bartalini, and P. D. Natale, *Opt. Lett.* **37**, 4811 (2012).
- [60] P. L. T. Sow, S. Mejri, S. K. Tokunaga, O. Lopez, A. Goncharov, B. Argence, C. Chardonnet, A. Amy-Klein, C. Daussy, and B. Darquié, *Appl. Phys. Lett.* **104**, 264101 (2014).
- [61] B. Argence, B. Chanteau, O. Lopez, D. Nicolodi, M. Abgrall, C. Chardonnet, C. Daussy, B. Darquié, Y. Le Coq, and A. Amy-Klein, *Nat. Photonics* **9**, 456 (2015).
- [62] M. Triches, M. Michieletto, J. Hald, J. K. Lyngsø, J. Lægsgaard, and O. Bang, *Opt. Express* **23**, 11227 (2015).
- [63] K. Knabe, S. Wu, J. Lim, K. A. Tillman, P. S. Light, F. Couny, N. Wheeler, R. Thapa, A. M. Jones, J. W. Nicholson, B. R. Washburn, F. Benabid, and K. L. Corwin, *Opt. Express* **17**, 16017 (2009).
- [64] M. Takiguchi, Y. Yoshikawa, T. Yamamoto, K. Nakayama, and T. Kuga, *Opt. Lett.* **36**, 1254 (2011).
- [65] A. Naumov, A. Podshivalov, K. Drabovich, R. Miles, and A. Zheltikov, *Phys. Lett. A* **289**, 207 (2001).
- [66] A. V. Shchegrov, K. Joulain, R. Carminati, and J.-J. Greffet, *Phys. Rev. Lett.* **85**, 1548 (2000).
- [67] J. J. Greffet, R. Carminati, K. Joulain, J. P. Mulet, S. Mainguy, and Y. Chen, *Nature (London)* **416**, 61 (2002).
- [68] A. Laliotis, T. Passerat de Silans, I. Maurin, M. Ducloy, and D. Bloch, *Nat. Commun.* **5**, 4364 (2014).

- [69] P. Todorov and D. Bloch, *J. Chem. Phys.* **147**, 194202 (2017).
- [70] O. A. Rabi, A. Amy-Klein, S. Saltiel, and M. Ducloy, *Europhys. Lett.* **25**, 579 (1994).
- [71] N. Skribanowitz, I. P. Herman, J. C. MacGillivray, and M. S. Feld, *Phys. Rev. Lett.* **30**, 309 (1973).
- [72] J. Guo, J. Cooper, and A. Gallagher, *Phys. Rev. A* **53**, 1130 (1996).